

Mineral control of organic carbon mineralization in a range of temperate conifer forest soils

CRAIG RASMUSSEN*, RANDAL J. SOUTHARD† and WILLIAM R. HORWATH‡

*Department of Soil, Water, and Environmental Science, University of Arizona, 520 Shantz Bldg., PO Box 210038, Tucson, AZ 85721, USA, †Land, Air and Water Resources Department, University of California, Davis, One Shields Ave, Davis, CA 95616, USA

Abstract

Coupled climate–ecosystem models predict significant alteration of temperate forest biome distribution in response to climate warming. Temperate forest biomes contain approximately 10% of global soil carbon (C) stocks and therefore any change in their distribution may have significant impacts on terrestrial C budgets. Using the Sierra Nevada as a model system for temperate forest soils, we examined the effects of temperature and soil mineralogy on soil C mineralization. We incubated soils from three conifer biomes dominated by ponderosa pine (PP), white fir (WF), and red fir (RF) tree species, on granite (GR), basalt (BS), and andesite (AN) parent materials, at three temperatures (12.5 °C, 7.5 °C, 5.0 °C). AN soils were dominated by noncrystalline materials (allophane, Al-humus complexes), GR soils by crystalline minerals (kaolinite, vermiculite), and BS soils by a mix of crystalline and noncrystalline materials. Soil C mineralization (ranging from 1.9 to 34.6 [mg C (g soil C)⁻¹] or 0.1 to 2.3 [mg C (g soil)⁻¹]) differed significantly between parent materials in all biomes with a general pattern of AN < BS < GR. We found significant negative relationships between Fe-oxyhydroxides, Al-oxyhydroxides, and Al-humus complex content and soil C mineralization, suggesting mineral control of C mineralization. Modeled decomposition rates and mineralizable pool size increased with increasing temperature for all parent materials and biomes. Further, $\delta^{13}\text{C}$ values of respired CO₂ suggest greater decomposition of recalcitrant soil C compounds with increasing temperature, indicating a shift in primary C source utilization with temperature. Our results demonstrate that soil mineralogy moderates soil C mineralization and that soil C response to temperature includes shifts in decomposition rates, mineralizable pool size, and primary C source utilization.

Keywords: Al-humus complex, climate change, first-order kinetics, short-range order minerals, soil carbon dynamics, soil mineralogy, temperate forest ecosystems

Received 22 April 2005; revised version received 18 November 2005 and accepted 1 December 2005

Introduction

The role of soils as a reservoir of carbon (C) and source of atmospheric CO₂ is an important aspect of the global C cycle. Soils contain approximately two-thirds of the terrestrial C budget, with estimates on the order of 1500–2000 Pg C (Anderson, 1995). Forested biomes contain a significant portion of this terrestrial soil C, both globally (Schlesinger, 1997) and regionally (e.g. the Pacific Northwest of the continental United States; Homann *et al.*, 1998). Coupled climate–ecosystem

models predict a general warming of temperate forest systems under future climate scenarios, combined with movement of low elevation biomes to higher elevations (NAST, 2000). For example, regional models suggest that temperate forests in the Sierra Nevada of California will move upward in elevation in response to climate warming, following their preferred climatic regime (Shafer *et al.*, 2001; Lenihan *et al.*, 2003).

Temperature change may affect soil C storage by altering decomposition rates and substrate utilization patterns. Simulation models generally assume a fixed mineralizable C pool that responds to temperature increases with a simple increase in decomposition rate or decomposition rate constant (Paul & Clark, 1996).

Correspondence: Craig Rasmussen, fax (520) 621 1647, e-mail: crasmuss@ag.arizona.edu

However, recent studies suggest that temperature change may also be accompanied by a change in mineralizable C pool size through greater access to recalcitrant soil C (Dalias *et al.*, 2001; Waldrop & Firestone, 2004). Mechanisms controlling pool size change may involve shifts in the active microbial community (MacDonald *et al.*, 1995; Zogg *et al.*, 1997; Zak *et al.*, 1999), with a concomitant shift in enzyme production or the biochemical pathways of mineralization (Andrews *et al.*, 2000; Waldrop & Firestone, 2004), or accumulation and protection of secondary microbial byproducts by the mineral soil matrix (Zunino *et al.*, 1982; Sagggar *et al.*, 1996; Dalias *et al.*, 2003).

Temperature driven changes in soil C dynamics and mineralizable pool size may be moderated in part by the mineral soil matrix and the physical protection of soil C. Current models of soil C dynamics generally use soil physical parameters, such as clay content, to partition soil C into pools of varying size and mean residence time (Parton *et al.*, 1987). However, substantial research indicates the soil mineral assemblage is more important than clay content in controlling soil C dynamics, particularly the presence of short-range-order materials and Al-humus complexes (Martin & Haider, 1986; Veldkamp, 1994; Torn *et al.*, 1997; Percival *et al.*, 2000). Mechanisms of organic C stabilization by the mineral matrix include: (i) direct adsorption of organics to mineral surfaces through entropy driven reactions; (ii) hydrophobic interactions, van der Waal's forces and H-bonding; (iii) or through multivalent cations (such as Ca^{2+} , Al^{3+} , and Fe^{3+}) that bridge the negative charge of mineral and organic surfaces (Stevenson, 1994). Adsorption to mineral surfaces imparts physical stability recalcitrance to soil C by making it inaccessible to the microbial community (Baldock & Skjemstad, 2000). In addition, aggregation of mineral particles through mineral-mineral or mineral-organic interactions may further stabilize organic C by occlusion of soil C within aggregate structures (Oades, 1988; Six *et al.*, 2000).

Short-range order (SRO) materials (minerals that lack long-range crystal atomic order) are prevalent in soils derived from volcanic parent materials and include SRO aluminosilicates (allophane and imogolite), SRO Fe-oxyhydroxides (ferrihydrite), SRO Al-oxyhydroxides, and Al-humus complexes (Shoji *et al.*, 1993). SRO materials possess tremendous reactive surface area (on the order of $800 \text{ m}^{-2} \text{ g}^{-1}$) (Harsh *et al.*, 2002) and exhibit variable charge due to an abundance of pH-dependent surface charge sites (Parfitt, 1980). At pH values below 6.5, SRO materials exhibit considerable anion exchange capacity or positively charged surface sites (Parfitt, 1980; Harsh *et al.*, 2002) that may interact with negatively charged organic functional groups. In addition,

organics may coordinate with surface Al and Fe groups, forming stable organo-mineral complexes (Tate & Theng, 1980; Yuan *et al.*, 2000). These properties facilitate protection of organic C directly through surface adsorption reactions and indirectly by promoting particle cementation and the formation of stable micro- and macroaggregate structures (Oades, 1988).

Soils with significant amounts of SRO materials tend to exhibit reduced C mineralization and greater soil C mean residence time than soils in similar environments lacking SRO materials (Zunino *et al.*, 1982; Sagggar *et al.*, 1994; Parfitt *et al.*, 2002). Enhanced stabilization and reduced turnover of soil C may be attributed to mineral aggregation and physical protection of existing soil C by mineral surfaces (Torn *et al.*, 1997; Rasmussen *et al.*, 2005), adsorption and deactivation of enzymes and microbial byproducts by SRO mineral surfaces (Sagggar *et al.*, 1994; Miltner & Zech, 1998), and co-precipitation of organics with SRO Al-oxyhydroxides and Al-humus complexes (Boudot, 1992; Schwesig *et al.*, 2003). In addition, Al-humus complexation may inhibit microbial decomposition through Al-toxicity (Tate & Theng, 1980; Illmer *et al.*, 2003), thereby promoting organic C accumulation.

Other studies have demonstrated significant variation in adsorption of C to crystalline and SRO mineral surfaces (Jardine *et al.*, 1989) and subsequent mineralization of adsorbed C (Jones & Edwards, 1998). For example, Jones & Edwards (1998) found decreased C adsorption capacity for illite and kaolinite minerals relative to ferrihydrite, a SRO Fe-oxyhydroxide. Furthermore, following adsorption, Jones & Edwards (1998) found that illite and kaolinite samples demonstrated greater mineralization of adsorbed C relative to ferrihydrite samples. The lack of soil C protection in systems dominated by kaolinite and mica-like 2:1 phyllosilicates (e.g. illite and vermiculite) may be due to reduced reactive surface area available for adsorption reactions that would physically protect soil C from microbial degradation. In particular, high charge vermiculite interlayers and interlayering with Al-OH, may sterically hinder adsorption of organic molecules in interlayer positions, effectively removing a significant area of potential adsorption sites (Guggenberger & Haider, 2002).

The objectives of this study were to quantify the influence of soil mineral assemblage on temperate forest soil C response to temperature in a range of Sierra Nevada conifer biomes. We were particularly interested in how the soil mineral assemblage controls the response of (i) total soil C mineralization, (ii) labile and resistant C pool sizes, (iii) soil C decomposition rates, and (iv) C source utilization to temperature. This research directly addresses how temperate forest soil C

dynamics may change with climate warming or changes in soil temperature.

Methods

Field setting

The western slope of the Sierra Nevada and southern Cascade Range provide an exceptional opportunity to study the effects of climate on soil C dynamics in soils from similar biomes, but with unique mineral assemblages. Climate and vegetative communities change consistently from low elevation to high elevation (Fig. 1 and Table 1). Precipitation increases and temperature decreases with increasing elevation, with these variables controlling the elevation distribution of each biome. The absolute elevation boundaries of each biome changes with latitude (e.g. biome elevation limits decrease with increasing latitude), following macroclimate variation. We sampled elevation transects across three conifer biomes (ponderosa pine (PP; *Pinus ponderosa* Laws.), white fir (WF; *Abies concolor* (Gord. and Glend.) Lindl.), and red fir (RF; *Abies magnifica* A. Murr.), on three parent materials (granite (GR), andesite (AN),

basalt (BS)) in the Sierra Nevada of California (Fig. 1). Biomes were named for the dominant overstory species and are referred to by a combination of parent material and biome name (e.g. andesite and ponderosa pine, ANpp, or basalt and red fir, BSrf).

Field sampling and soil analysis

Three pedons, separated by approximately 10 m, were sampled at each biome field site. We constrained sampling sites to similar landforms (summit locations), similar slope (<10%), similar aspect (W and SW facing slopes), and similar canopy position (outside of tree canopy) in order to minimize landscape and microclimate variability between sites. Samples were collected from each pedon by morphologic horizon as designated in the field. Collected samples were air dried and sieved to <2 mm, and all further analyses performed on the <2 mm fraction.

Particle size analysis was determined by the pipette method (Jackson, 1975). Samples for clay content were pretreated with sodium hypochlorite to remove organic matter and dispersed in sodium-hexametaphosphate. Dispersed samples were wet sieved at 53 µm and clay

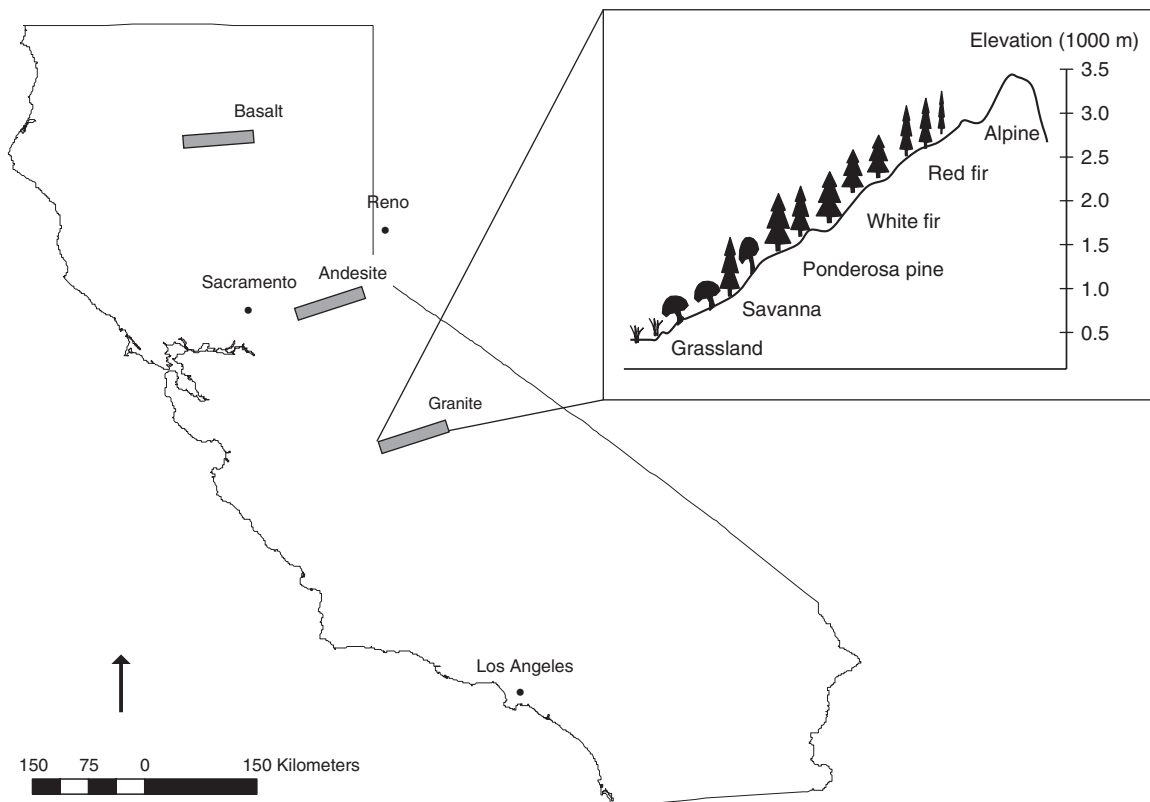


Fig. 1 Transect locations on the western slope of the Sierra Nevada. Inset shows the change in biomes with elevation. Similar vegetation sequences exist at each transect location. Scale bar is for California.

Table 1 Dominant vegetation and climate parameters (\pm SE) for selected conifer biomes across the western slope of the California Sierra Nevada

Biome	Dominant vegetation	Elevation limits (m)		MAP (cm yr^{-1})	MAST ($^{\circ}\text{C}$)	Incubation MAST ($^{\circ}\text{C}$)
		Lower	Upper			
PP	<i>Pinus ponderosa</i> <i>Pinus lambertiana</i> <i>Quercus kelloggii</i> <i>Calocedrus decurrens</i>	900	1500	103 (12)	13.6 (0.3)	12.5
WF	<i>Abies concolor</i> <i>Pinus ponderosa</i> <i>Pinus lambertiana</i>	1500	2100	115 (10)	9.1 (0.9)	7.5
RF	<i>Abies magnifica</i> <i>Pinus jeffreyi</i>	2100	2600	135 (9)	6.7 (0.3)	5.0

Biome abbreviations are as follows: PP, ponderosa pine; WF, white fir; RF, red fir. Dominant vegetation is listed in order of overstory dominance.

Mean annual precipitation (MAP) and mean annual soil temperature (MAST) values estimated from 30 year average climate data (1971–2000) from the PRISM climate dataset (<http://www.ocs.orst.edu/prism/>).

Incubation MAST is the temperature used to represent the MAST for each biome for incubation experiments.

and silt collected in 1 L cylinders for pipette analysis. Total organic C, N, and ^{13}C were measured for each horizon using a combination of high-temperature dry combustion (Carlo-Erba Elemental Analyzer, CE Elantech Inc., Lakewood, NJ, USA), and continuous flow Isotope Ratio Mass Spectrometry (Europa Hydra 20/20, PDZ Europa, Cheshire, UK). Soils did not react with HCl and, therefore, were not pretreated to remove carbonates. All mass percent calculations were corrected for air dry water content.

Mineralogy

Qualitative mineralogical analysis by X-ray diffraction (XRD) was conducted on the clay ($<2\mu\text{m}$) fraction of one pedon from each sample site. Clay size material was collected from the particle size analysis with repeated mixing and centrifugation in dilute Na_2CO_3 . X-ray analyses were made with a Diano XRD 8000 diffractometer (Diano, Woburn, MA, USA) producing $\text{Cu-K}\alpha$ radiation. Clays were oriented and mounted on glass slides with the following standard treatments: Mg-saturation, Mg-saturation/glycerol solvation, K-saturation, and heat treatment of K-saturated samples at 350°C and 550°C (Whittig & Allardice, 1986).

Quantitative mineralogical analysis of bulk soil by selective dissolution procedures was performed using standard methods of acid ammonium-oxalate, sodium-pyrophosphate, and citrate dithionite extraction (National Soil Survey Laboratory, 1996). Extractions were not sequential. Oxalate extracts Al, Fe, and Si (Al_o , Fe_o , Si_o) from organic complexes and SRO Fe-oxyhydroxides

(e.g. ferrihydrite) and aluminosilicates (e.g. allophane and imogolite). Pyrophosphate extracts Al (Al_p) bound in organo-metal complexes. Sodium dithionite extracts Fe (Fe_d) from organic complexes, and secondary forms of Fe-oxyhydroxides, both crystalline and noncrystalline (Parfitt & Childs, 1988; Dahlgren, 1994). Si, Al, and Fe were measured by atomic absorption (AA) spectrometry (AA8000, Perkin-Elmer, Wellesley, MA, USA). Si and Al AA spectrometry analyses were conducted using a mixed acetylene-nitrous oxide flame. Allophane content was estimated from the Si_o content according to the $[(\text{Al}_o - \text{Al}_p)/\text{Si}_o]$ molar ratio (Dahlgren, 1994). Allophane content for samples with Al/Si molar ratios greater than 2.5 were not estimated, as the high ratio suggests extraction of Al from species other than allophane, such as Al-oxyhydroxide species in mineral interlayers or on mineral surfaces (Dahlgren, 1994).

Incubation design

Soil material from each biome (PP, WF, RF) was incubated at three different temperatures (5.0°C , 7.5°C , and 12.5°C), in order to quantify soil C response to temperature. Incubation temperatures are representative of the mean annual soil temperature (MAST) for the RF, WF, and PP biomes, respectively (Table 1). The temperature sequences in the RF and WF soils may also be used to simulate climate warming, and a shift of climate parameters upward in elevation. For example, PP climate conditions move into WF or RF soils (e.g. 7.5 – 12.5°C or 5.0 – 12.5°C) and WF climate conditions move into RF soils (e.g. 5.0 – 7.5°C). The PP biome was used as a base-

line, in that we simulated a movement of PP MAST into WF and RF biomes and a movement of WF MAST into RF soils, but we did not simulate movement of lower elevation temperatures into the PP biome or movement of RF temperatures into higher elevation systems.

Incubation procedures

Soil material from the A horizons of the three pedons sampled at each site was composited for incubation. Four replicate samples (30 g of air dry soil) of the composited material were placed in specimen cups and brought to 55–60% of field capacity with deionized (DI) water. Specimen cups were placed in one quart Mason jars with septa to allow for headspace sampling. Soil moisture was maintained during the incubation by the addition of DI water to a depth of 0.5 cm in the bottom of the Mason jar, to maintain 100% relative humidity in the jars.

After wetting, all temperature treatment samples were allowed to 'preincubate' for 5 days at room temperature ($\sim 23^\circ\text{C}$) before being placed in the appropriate temperature-controlled chamber, in order to initialize microbial activity. After this 'preincubation' period, each sample was mixed with a spatula, tamped down to a uniform depth and bulk density with a glass rod, and placed in dark, temperature-controlled chambers.

Mineralized CO_2 was measured on a frequent basis using an Infra-Red Gas Analyzer (Quibit CO_2 Analyzer, Model S-151, Quibit Systems, Kingston, ON, Canada). Sample jars were aired out after each sample period. Blank jars were also recorded to correct samples for background atmospheric CO_2 concentration. Gas samples for ^{13}C isotopic analyses were collected at 15-day intervals starting on day 5 of the incubation. Twelve milliliters of headspace atmosphere were extracted with a syringe, placed into a vacuum evacuated tube and analyzed for ^{13}C content, coincident with headspace CO_2 measurements. ^{13}C was measured by mass spectrometry (Europa Geo 20/20, PDZ Europa) and reported on a per mil basis using the standard convention relative to the Pee Dee Belemnite standard (Balesdent & Mariotti, 1996).

Calculation of CO_2 evolution at each sample period followed Zibilske (1994). Percent CO_2 was converted to a mass of C and expressed on a per gram soil (soil basis) [$\text{mg C (g soil)}^{-1}$], and normalized to soil C content (C activity basis) [$\text{mg C (g soil C)}^{-1}$]. The soil basis provides an estimate of the total mineralizable C pool, whereas the C activity basis provides an estimate of the fraction of soil C that was mineralized.

Statistical methods

We used nonlinear regression to fit first-order decay models to C mineralization rate data. C mineralization

data were grouped into discrete points for analysis of mineralization rates as suggested by Hess & Schmidt (1995). The use of discrete rate data overcomes errors associated with fitting first-order models to cumulative CO_2 production (Ellert & Bettany, 1988; Taylor & Parkinson, 1988; Hess & Schmidt, 1995). The model that gave the best fit for the majority of the rate data consisted of two pools, what we termed a labile pool and a resistant pool, following first-order decay reactions:

$$-dC/dt = C_L e^{-k_L t} + C_R e^{-k_R t}, \quad (1)$$

where dC/dt is [$\text{mg C (g soil C)}^{-1} \text{ day}^{-1}$], C_L and C_R are the decomposition rates of the labile (C_L) and resistant (C_R) pools at time $t = 0$ [$\text{mg C (g soil C)}^{-1} \text{ day}^{-1}$], and k_L and k_R are curve fitting constants that represent decomposition rate constants (day^{-1}) for each pool. Model parameters C_L , C_R , k_L , and k_R were determined using a least-squares estimate approach with iterative adjustment of curve variables to achieve the best fit (Devevre & Horwath, 2000; Dalias *et al.*, 2001). Initially, we fit all model parameters without constraints and found k_R to be similar for all samples. Following the initial model parameterization, we fixed k_R at 0.001 for all samples and recalculated model parameters. Model estimation was performed using the nonlinear model module in JMP IN 5.1 (SAS Institute, Cary, NC, USA).

We found significant improvement in fitting the rate data with a two compartment models vs. a one compartment model as evidenced by improved adjusted R^2 values, a reduction in residual sums of squares and by using an F -test to compare residual sums of squares and degrees of freedom between the two models (Dalias *et al.*, 2001). Model residuals also showed random patterns over time suggesting minimal bias in the regression model (Hess & Schmidt, 1995).

Pool size was estimated by integrating the area under the curve for both labile and resistant pools:

$$C_{Ti} = C_i / -k_i (e^{-k_i t} - 1), \quad (2)$$

where C_{Ti} is the pool size of each respective pool ($i = \text{labile (L) or resistant (R)}$) [$\text{mg C (g soil C)}^{-1}$] and C_i and k_i are as noted in Eqn. (1).

We tested for differences in soil properties and C mineralization between the factorial combination of parent material (AN, BS, GR) and biome (PP, WF, RF) using a one-way ANOVA and Tukey's HSD *post hoc* test ($P \leq 0.05$). Linear regression analysis between cumulative CO_2 production (on a C activity basis), mineralogical properties (clay content, and selective dissolution extracts) and litter quality properties (C/N, ^{13}C of soil C) at each temperature (5.0°C , 7.5°C , and 12.5°C) was used to examine the influence of mineralogy on CO_2 mineralization. AN, GR, and BS samples were pooled

Table 2 Soil taxonomic classification for conifer biome sample sites in the California Sierra Nevada

Biome	Parent material	Soil classification
PP	GR	Fine-loamy, mixed, semiactive, mesic Ultic Haploxeralf
	BS	Fine, kaolinitic, mesic Xeric Haplohumult
	AN	Fine, parasesquic, mesic Andic Palehumult
WF	GR	Coarse-loamy, mixed, superactive, mesic Humic Dystroxerept
	BS	Loamy-skeletal, mixed, superactive, mesic Typic Haploxerept
	AN	Medial-skeletal, amorphic, mesic Humic Haploxerand
RF	GR	Mixed, superactive, frigid Dystric Xeropsamment
	BS	Sandy-skeletal, mixed, superactive, frigid Typic Xerorthent
	AN	Medial-skeletal, amorphic, frigid Humic Vitrixerand

Biome and parent material abbreviations are as follows: PP, ponderosa pine; WF, white fir; RF, red fir; GR, granite; BS, basalt; AN, andesite.

Soil classification based on Soil Taxonomy, 9th edn, USDA Soil Survey Staff (2003).

for regression analyses ($n = 36$). Regression and ANOVA analyses were performed with JMP IN 5.1 (SAS Institute).

Results and discussion

Soil characterization data

Soils were of similar taxonomic unit within each biome across parent materials (Table 2). Soils progress from highly weathered soils with significant subsurface clay accumulation (Ultisols and Alfisols) in the PP biome, to soils that lack significant clay accumulation or diagnostic horizon development (Andisols and Inceptisols) in the WF biome, to soils lacking any significant degree of pedogenesis (Entisols and Andisols) in the RF biome. The change in weathering intensity and soil development with elevation is related to temperature and the dominant form of precipitation (e.g. rain or snow), with colder temperatures and snowfall limiting chemical and physical weathering in WF and RF biomes (Dahlgren *et al.*, 1997).

Crystalline (Fe_d) and SRO Fe-oxyhydroxide (Fe_o), SRO Al-oxyhydroxide (Al_o), SRO aluminosilicate (allophane), and Al-humus (Al_p) complex content varies significantly between parent materials within each biome (Table 3). In addition, there are substantial qualitative differences in the crystalline mineral assemblage as indicated by XRD analyses (Table 3). GR soils are distinct from AN and BS soils in that they lack any significant accumulation of SRO materials and contain vermiculite or hydroxy-interlayered vermiculite (HIV) in each biome. AN and BS soils contain similar crystalline clay minerals, although BS biomes tend to exhibit a greater proportion of hydroxy-interlayered smectite (HIS) minerals, whereas AN soils tend to be dominated by SRO minerals. AN soils, in particular ANwf and

ANrf, contain significantly greater amounts of SRO Fe-oxyhydroxides, SRO aluminosilicates, and Al-humus complexes, relative to GR and BS biomes (Table 3).

In general, pH values are more acid in GR soils relative to BS and AN, with the greatest pH values in BS biomes (Table 3). This is not unexpected and may be related to the mineral composition of the parent materials; with GR parent material dominated by felsic minerals (quartz and feldspar) that provide limited 'base cations' upon weathering and subsequently limited pH buffering capacity; whereas BS parent material is dominated by mafic minerals (hornblende, olivine, plagioclase) that provide substantial base cations and pH buffering capacity. It is interesting to note the variation in pH between BSwf and ANwf biomes, both of which are dominated by SRO materials that contain substantial pH-dependent charge. The variation in pH potentially impacts mineral surface charge (BS soils with greater negative charge; AN soils with greater positive charge) and the related protective capacity of the SRO minerals in each respective parent material (Parfitt, 1980).

Soil C exhibits minimal variation between parent materials and biomes, whereas C/N and ^{13}C values exhibit significant differences (Table 3). In general, AN and BS soils contain greater soil C relative to GR, although differences are not significant. The BSrf biome contains the greatest C on a mass percent basis (161 g kg^{-1}) relative to any of the other biomes. In the field, the BSrf surface horizon (0–3 cm) was classified as an A1 horizon, but subsequent analysis of C content determined that this horizon actually contains greater than 20% C, which would lead to its classification as an Oa horizon (Soil Survey Staff, 2003). Using this material in the incubation experiment skewed the patterns of CO_2 production from this biome, and will be discussed in further detail below.

Table 3 Soil characterization data (\pm SE) for A horizon soil material collected from sample sites and used for laboratory incubation studies

Biome	Parent material	Basic soil properties		Organic carbon variables				Mineralogy variables						Clay mineralogy
		Depth (cm)	pH H ₂ O	Clay (g kg ⁻¹)	C (g kg ⁻¹)	C/N	$\delta^{13}\text{C}$ (‰)	Fe _d (g kg ⁻¹)	Fe _o (g kg ⁻¹)	Si _o (g kg ⁻¹)	Al _o (g kg ⁻¹)	Al _p (g kg ⁻¹)	Allophane (g kg ⁻¹)	
PP	GR	0-7	5.4	140	65 (2.6) ^b	24 (0.1) ^{bc}	-27.7 (0.6) ^e	5.6 (0.8) ^{ef}	1.2 (0.1) ^c	1.0 (0.6) ^c	2.5 (0.9) ^e	1.4 (0.4) ^d	5	K > V
	BS	0-7	6.2	268	70 (7.3) ^b	24 (0.5) ^{bc}	-26.4 (0.2) ^{cd}	46.3 (1.0) ^a	2.6 (0.2) ^{bc}	1.8 (0.1) ^c	8.4 (0.4) ^{cd}	4.5 (0.4) ^c	12	K > > S > Go = G
	AN	0-6	6.0	254	98 (7.1) ^{ab}	29 (0.8) ^a	-27.0 (0.2) ^{de}	26.6 (1.5) ^b	3.1 (0.1) ^b	2.8 (0.5) ^c	8.9 (0.6) ^c	4.4 (0.3) ^c	17	K > G > HIS
WF	GR	0-13	6.0	77	51 (9.9) ^b	23 (0.5) ^{bc}	-25.5 (0.1) ^b	4.4 (0.1) ^{ef}	2.8 (0.3) ^{bc}	1.1 (0.1) ^c	6.4 (1.0) ^{cd}	2.7 (0.8) ^{cd}	—	HIV > K > > G
	BS	0-10	6.5	63	93 (14) ^{ab}	20 (1.5) ^{cd}	-25.7 (0.3) ^{bc}	7.0 (0.4) ^e	2.7 (0.2) ^{bc}	9.9 (1.7) ^{ab}	17.9 (2.1) ^b	7.6 (0.6) ^b	50	SRO > > HIS > K = G
	AN	0-11	5.8	94	84 (2.4) ^{ab}	25 (0.5) ^b	-24.1 (0.1) ^a	18.6 (1.3) ^c	6.8 (0.4) ^a	11.2 (0.5) ^a	31.7 (0.7) ^a	10.5 (0.1) ^a	78	SRO > > G = K
RF	GR	0-8	5.5	87	53 (18) ^b	30 (1.4) ^a	-23.9 (0.2) ^a	5.2 (0.1) ^{ef}	3.9 (0.4) ^b	0.2 (0.0) ^c	3.5 (0.3) ^{de}	2.5 (0.3) ^{cd}	—	G > K = HIV
	BS	0-8	5.8	67	161 (45) ^a	20 (0.7) ^{cd}	-25.7 (0.3) ^{bc}	3.1 (0.3) ^f	2.3 (0.1) ^{bc}	0.7 (0.3) ^c	2.5 (0.4) ^e	1.7 (0.1) ^d	4	K = HIS > SRO
	AN	0-11	5.5	77	97 (33) ^{ab}	30 (3.6) ^a	-24.4 (0.1) ^a	13.1 (0.3) ^d	5.2 (0.1) ^a	7.7 (0.2) ^b	27.0 (1.1) ^a	8.3 (0.8) ^{ab}	54	SRO > > HIS = K

Depth values represent horizon depths as sampled in the field. pH and clay values represent one data point collected for composite soil samples used in the incubation.

Organic carbon and mineralogy variables represent average values of the three pedons sampled at each field site ($n = 3$). Significance was determined using one-way ANOVA's followed by Tukey's HSD *post hoc* tests, where conditions of normality and homogeneity of variance were met; within each of the columns, means followed by different letters are significantly different from each other at $P \leq 0.05$.

Allophane content estimated from the Al_o-Al_p/Si_o molar ratio based on Dahlgren (1994). Clay mineralogy was determined by X-ray diffraction and minerals are listed in order of relative abundance based on relative peak intensity in X-ray diffractograms.

Abbreviations are as follows: G, gibbsite; HIS, hydroxy interlayered smectite; HIV, hydroxy interlayered vermiculite; K, kaolinite/halloysite; SRO, short-range order; V, vermiculite; PP, ponderosa pine; WF, white fir; RF, red fir; GR, granite; BS, basalt; AN, andesite.

C/N values are generally greatest in AN, and least in BS soils in each respective biome (Table 3). The greatest difference between parent materials is in the RF biome where AN and GR soils exhibit significantly greater values (C/N = 30 for each parent material) than BS soils (C/N = 20). Variation in C/N within a biome between parent materials suggests soil C quality and decomposability may vary with parent material. Soil C ^{13}C values tend to become enriched with increasing elevation in all parent materials, with RF biomes generally three per mil enriched relative to PP biomes (PP soil C ^{13}C averages of -27.0 across parent materials compared with RF soil C ^{13}C average of -24.5 across parent materials). Variation in soil C ^{13}C may be due to differences in the ^{13}C of litter inputs or variation in soil C quality resulting from variability in water and N.

Soil C mineralization by biome

Soil CO_2 production varied significantly between parent materials and biomes (Table 4). GR soils produced the most CO_2 on a C activity basis, followed by BS, and AN soils. Significant variation in CO_2 production between parent materials suggests differences in soil mineralogy significantly effects soil C mineralization. In addition, CO_2 production varied significantly between biomes (PP > WF > RF), suggesting variation in soil properties or litter quality impacts soil C mineralization (Table 4). Specific differences between parent materials by biome and temperature are examined below.

On a soil basis, GRpp soils produced more CO_2 than ANpp and BSpp biomes at each temperature, whereas ANpp and BSpp soils produced similar amounts of CO_2 (Table 5). Differences in soil C mineralization were more pronounced on a C activity basis, with GRpp soils mineralizing from two to four times as much C relative to ANpp and BSpp soils at each temperature. These results suggest GRpp soil C is extremely labile and sensitive to temperature relative to BSpp and ANpp soil C, with ANpp having the most recalcitrant soil C pools. GRpp soils contain appreciable amounts of vermiculite in the clay fraction (Table 3) that may account for the lack of protection of GRpp soil C (Jardine *et al.*, 1989; Jones & Edwards, 1998).

In the WF biome, BSwf soils produced greater CO_2 than GRwf and ANwf biomes on a soil basis at each temperature (Table 5). Overall CO_2 production was minimal in the ANwf soils (less than half of the CO_2 produced in GRwf and BSwf soils), suggesting recalcitrant soil C pools. ANwf soils contain substantial amounts of allophane and Al-humus complexes (Table 3) that may account for the recalcitrance of these soil C pools. On a C activity basis, GRwf soils mineralized

Table 4 Mean cumulative CO_2 (\pm SE) respired, reported for each factor (parent material and biome)

Factor	Cumulative CO_2 [mg C (g soil C) $^{-1}$]
Parent material	
GR	15.0 (1.5) ^a
BS	8.3 (0.6) ^b
AN	4.8 (0.5) ^c
Biome	
PP	14.2 (1.6) ^a
WF	7.7 (0.8) ^{ab}
RF	6.1 (0.5) ^b

Significance was determined by one-way ANOVA using a full factorial model (including parent material, biome, and the parent material \times biome interaction) followed by Tukey's HSD *post hoc* tests; within each factor, means followed by different levels are significantly different from each other at $P \leq 0.05$.

Means and significance for the parent material \times biome interaction are not reported.

PP, ponderosa pine; WF, white fir; RF, red fir; GR, granite; BS, basalt; AN, andesite.

more soil C than BSwf and ANwf soils. ANwf soil C mineralization was three to four times less than BSwf and GRwf soils, respectively, again suggesting ANwf soil C is extremely recalcitrant, with only a small fraction of labile C relative to the other parent materials. Greater GRwf CO_2 production on a C activity suggests that while overall (on a soil basis), GRwf soils produced less CO_2 , a greater percentage of the existing GRwf soil C is more labile and sensitive to temperature than the respective BSwf and ANwf soil C pools. The large labile C component in the GRwf soils may be directly related to soil mineralogy and the lack of SRO minerals to physically protect soil C. BSwf and ANwf exhibit relatively similar soil mineral assemblages with considerable SRO content (Table 3), but dramatically different overall soil C mineralization. The variation in soil C mineralization may be related to soil pH and protonation of SRO material pH-dependent charge sites. At pH 6.5, BSwf SRO materials may be near their zero point of charge (Parfitt, 1980) and exhibit minimal positive charge for surface adsorption of organics, thereby limiting the protection capacity of these minerals.

CO_2 production in the RF biome was greatest in BSrf soils on a soil basis at each temperature (Table 5), likely a function of the relatively high soil C content of these soils (Table 3). In comparison, on a C activity basis, GRrf soils mineralized more soil C than BSrf and ANrf soils at each temperature. As with the PP and WF biome, greater GRrf soil C mineralization on a C activity basis suggests a greater portion of the GRrf soil C is labile

Table 5 Cumulative soil CO₂ respired and decomposition model parameters for each biome, parent material, and temperature treatment

Biome	Temperature (°C)	Parent material	Cumulative CO ₂ respired			Rate model parameters			
			Soil basis [mgC (g soil) ⁻¹]	C activity basis [mgC (g soil) ⁻¹]	k _L (day ⁻¹)	C _L [mgC (g soil) ⁻¹ day ⁻¹]	C _R [mgC (g soil) ⁻¹ day ⁻¹]	C _{TL} [mgC (g soil) ⁻¹]	C _{TR}
PP	12.5	GR	2.3	34.6	0.017	0.889	0.000	41.0	0.0
	12.5	BS	1.0	14.7	0.092	0.243	0.152	2.7	12.7
	12.5	AN	1.1	10.9	0.053	0.210	0.096	3.9	7.9
	7.5	GR	1.6	24.1	0.197	0.424	0.281	2.2	24.2
	7.5	BS	0.6	8.6	0.404	0.267	0.101	0.7	8.3
	7.5	AN	0.6	6.2	0.037	0.097	0.053	2.5	4.4
	5.0	GR	1.1	16.9	0.193	0.263	0.158	1.4	13.6
	5.0	BS	0.5	6.6	0.388	0.173	0.082	0.4	6.8
	5.0	AN	0.5	5.3	0.030	0.081	0.039	2.5	3.2
WF	12.5	GR	0.8	16.4	0.030	0.339	0.099	10.6	8.5
	12.5	BS	1.1	12.1	0.088	0.362	0.105	4.1	8.8
	12.5	AN	0.4	4.6	0.048	0.061	0.044	1.3	3.6
	7.5	GR	0.5	10.4	0.108	0.189	0.114	1.7	9.8
	7.5	BS	0.7	7.8	0.158	0.241	0.085	1.5	7.0
	7.5	AN	0.2	2.4	0.010	0.020	0.012	1.2	1.0
	5.0	GR	0.5	9.0	0.138	0.135	0.079	1.0	6.8
	5.0	BS	0.4	4.7	0.070	0.043	0.033	0.6	2.8
	5.0	AN	0.1	1.9	0.011	0.020	0.010	1.1	0.8
RF	12.5	GR	0.6	10.9	0.068	0.028	0.125	0.4	10.7
	12.5	BS	1.6	9.7	0.110	0.153	0.106	1.4	8.9
	12.5	AN	0.7	6.6	0.099	0.073	0.075	0.7	6.2
	7.5	GR	0.4	6.8	0.172	0.073	0.077	0.4	6.6
	7.5	BS	0.9	5.7	0.151	0.111	0.064	0.7	5.5
	7.5	AN	0.3	3.0	0.681	0.142	0.034	0.2	2.8
	5.0	GR	0.3	5.7	0.133	0.071	0.039	0.5	3.4
	5.0	BS	0.7	4.4	0.262	0.104	0.052	0.4	4.3
	5.0	AN	0.2	1.9	0.681	0.076	0.024	0.1	2.0

Reported values for cumulative CO₂ respired represent the mean of four composite samples. As such, we do not report standard error or significance because as these values would only report procedural error and cannot be used to compare between treatments.

Rate model parameters were estimated assuming two pool first-order decay equation parameters for CO₂ mineralization rate over time: $-dC/dt = C_L e^{-k_L t} + C_{RE} e^{-k_R t}$, k_R fixed at 0.001.

Pool size of the labile and resistant pools were estimated by integrating the first-order decay equation for each pool: $C_{TR} = C_i/k_i (e^{-k_i t} - 1)$.

PP, ponderosa pine; WF, white fir; RF, red fir; GR, granite; BS, basalt; AN, andesite.

relative to BSrf and ANrf soil C. ANrf and BSrf soils are dominated by SRO minerals, whereas GRrf soils are dominated by HIV, kaolinite, and gibbsite (Table 3). The relative lack of protection of GRrf soil C may be directly related to the lack of SRO minerals.

Overall, cumulative biome CO₂ production suggests dramatic differences in soil C mineralization that may be related to parent material and soil mineralogy. AN soil C appears to be very recalcitrant relative to BS and GR soils, suggesting soil C stocks in these biomes may be well buffered against temperature and that AN soils are more likely to preserve their current soil C stocks under climate warming conditions. In contrast, GR soil C is very labile and sensitive to temperature, suggesting that under climate change conditions, GR soil C stocks could be significantly affected. We suggest the variation in soil C mineralization is driven by soil mineral assemblage characteristics. In order to test this hypothesis, specific relationships between soil mineral variables and soil C mineralization were examined using regression analyses (see below).

Mineral assemblage and soil C quality control of soil C mineralization

Regression analysis was used to directly examine the relationship between soil C mineralization, soil mineral properties, and soil C quality indicators (C/N and $\delta^{13}\text{C}$). This analysis suggests highly significant negative relationships between SRO Fe-(Fe_o) and Al-oxyhydroxide (Al_o-Al_p), and Al-humus complex (Al_p) content and CO₂ production at each incubation temperature (Table 6). This is in accord with previous studies indicating a high correlation between stable soil C content and SRO minerals (Veldkamp, 1994; Shang & Tiessen, 1998; Percival *et al.*, 2000; Rasmussen *et al.*, 2005), suggesting a significant role for SRO minerals in controlling soil C dynamics. It is interesting to note, SRO Fe-oxyhydroxides, are consistently highly and negatively correlated with soil C mineralization across temperature treatments (Table 6), indicating a temperature-independent control of these minerals on C mineralization. In contrast, the negative correlation between SRO Al-oxyhydroxides, and Al-humus complexes and soil C mineralization increases as temperature decreases (Table 6), suggesting Al species play a larger role in controlling C mineralization at cold temperatures. The reason for this apparent shift in C mineralization controlling factors is unclear, but may be related to changing microbial community structure and rates of enzyme production with temperature (Zak *et al.*, 1999; Dalias *et al.*, 2001; Waldrop & Firestone, 2004) or possibly a greater Al-toxicity effect to the microbial community at colder temperatures.

Table 6 Regression analysis between cumulative CO₂ mineralized and soil mineral and soil C quality variables at each incubation temperature

Temperature (°C)	Equation	R _a ²	P-value
12.5	ln CO ₂ = 1.48–0.129(Fe _o)	0.77	<0.0001
	ln CO ₂ = 1.24–0.024(Al _o -Al _p)	0.55	<0.0001
	ln CO ₂ = 1.34–0.057(Al _p)	0.52	<0.0001
	ln CO ₂ = –2.61–0.141($\delta^{13}\text{C}$)	0.55	<0.0001
7.5	ln CO ₂ = 1.33–0.155(Fe _o)	0.79	<0.0001
	ln CO ₂ = 1.05–0.030(Al _o -Al _p)	0.57	<0.0001
	ln CO ₂ = 1.17–0.068(Al _p)	0.53	<0.0001
	ln CO ₂ = –3.43–0.166($\delta^{13}\text{C}$)	0.52	<0.0001
5	ln CO ₂ = 1.21–0.158(Fe _o)	0.78	<0.0001
	ln CO ₂ = 0.95–0.033(Al _o -Al _p)	0.67	<0.0001
	ln CO ₂ = 1.08–0.076(Al _p)	0.62	<0.0001
	ln CO ₂ = –3.53–0.168($\delta^{13}\text{C}$)	0.49	<0.0001

Regressions calculated on pooled data for AN, BS, and GR soils (*n* = 36).

Values for CO₂ are in units of [mg C (g soil C)⁻¹].

Values for soil mineral variables are in units of [g kg⁻¹].

Al_o-Al_p represents SRO Al-OH species minus Al-humus complexes.

GR, granite; BS, basalt; AN, andesite; SRO, short-range order.

Mineral control of CO₂ mineralization is particularly evident in ANwf soils that mineralized substantially less CO₂ than any other biome at each temperature (Table 5). The decreased mineralization appears to be directly related to SRO mineral and Al-humus complex content (Tables 3 and 6). In contrast, GR biomes, dominated by crystalline minerals and minimal SRO mineral content (Table 3), exhibited greater C mineralization for all biome and temperature combinations on a C activity basis (Table 5). The lack of SRO minerals and the presence of HIV and vermiculite species in the GR soils may reduce the protective capacity of the GR soil matrix (Jardine *et al.*, 1989; Jones & Edwards, 1998; Guggenberger & Haider, 2002).

Soil C quality indicators demonstrated varying relationships with C mineralization. Soil C/N did not exhibit any significant correlation with soil C mineralization for any of the temperature treatments (data not shown). In contrast, soil C ¹³C did exhibit a negative correlation with soil C mineralization, in that soils with enriched ¹³C signatures respired less CO₂ than soils with depleted ¹³C signatures (Table 6). However, including $\delta^{13}\text{C}$ as a variable with Fe_o in a multiple linear regression analysis only slightly improved the adjusted R² at each temperature (R_a² = 0.80, 0.82, and 0.82 for the 5.0 °C, 7.5 °C, and 12.5 °C treatments, respectively) and

Fe_o dominated the relationship as indicated by parameter *F*-values and sums of squares (data not shown).

Soil C mineralization kinetics by biome

In addition to substantial variation in cumulative C mineralization, modeled soil C dynamics vary considerably between parent materials within each biome, suggesting soil mineralogy may also affect rates of decomposition and the partitioning of soil C into labile and resistant pools (Table 5). As expected, all biomes and parent materials exhibit an increase in total soil C mineralized with increasing temperature (Table 5). We did not fix the size of the labile or resistant pool in modeling mineralization rate dynamics, so that as the total amount of mineralized C changes with temperature, the size of the modeled labile and resistant pools also changes. The relative change in each pool size provides a means of comparing C mineralization dynamics across parent materials and temperatures.

In the PP biome, the initial decomposition rates of labile and resistant pools (C_L and C_R , respectively) tend to increase with an increase in temperature. GRpp biomes exhibit the highest initial decomposition rates, particularly in the labile pool, where GRpp rates are two to four times greater than BSpp and ANpp C_L at each temperature. In conjunction with greater CO₂ mineralization at warmer temperatures (Table 5), modeled labile and resistant pool size (C_{TL} and C_{TR} , respectively) also increase considerably with an increase in temperature in the PP biome, suggesting mineralizable pool size varies with temperature. In particular, GRpp C_{TL} is approximately 20 times greater at 12.5 °C than 7.5 °C, with all mineralized C modeled to be sourced from the C_{TL} . This dramatic change in modeled dynamics suggests a temperature related shift in soil C utilization or possibly a shift in the active microbial community and microbial metabolism (e.g. Zogg *et al.*, 1997; Waldrop & Firestone, 2004). The data also suggest very little protection of GRpp soil C pools under warmer temperature scenarios, with soil C that at cold temperatures was modeled as resistant, now modeled in one fast turnover pool. ANpp soils exhibit relatively low initial decomposition rates and have a minimal increase in C_{TL} with an increase in temperature. Low decomposition rates and minimal change in labile pool size, suggest the ANpp soils are buffered against temperature effects on soil C mineralization, with the majority of the increase in C mineralization sourced from resistant soil C pools. These results are in agreement with previous studies indicating that the majority of surface horizon C in GRpp biomes turns over very rapidly (Trumbore *et al.*, 1996), whereas ANpp biomes demonstrate significant protection of soil C stocks (Ras-

mussen *et al.*, 2005). The difference in soil C dynamics is most likely related to mineralogy moderated soil C protection as discussed above.

WF biome kinetic models indicate increasing decomposition rate and pool size with increasing temperature for all parent materials. Both GRwf and BSwf C_{TL} increase substantially between 7.5 °C and 12.5 °C, indicating a greater proportion of total mineralized C in the labile pool. The change in pool size may be a function of a shift in microbial metabolism and enzyme production allowing for rapid utilization of C that was recalcitrant C at colder temperatures. In contrast, ANwf soils demonstrate minimal change in C_{TL} under climate change conditions, but a dramatic increase in C_L , suggesting rapid utilization of a fixed labile pool. The fixed pool size may be a function of protection of soil C by SRO minerals and decreased substrate availability, or an inhibition of microbial enzyme efficiency because of enzyme adsorption to mineral surfaces (Miltner & Zech, 1998).

RF biomes appear to be dominated by resistant soil C pools (C_{TR}), with the majority of mineralized C sourced from C_{TR} in all of the parent materials. GRrf soils respond differently than BSrf, ANrf, and the other GR biomes to temperature increase in terms of C_L and C_{TL} . Although GRrf soils mineralized the greatest amount of soil C relative to BSrf and ANrf soils, GRrf C_{TL} appears to be fixed, with increased CO₂ mineralization sourced from resistant pools. In contrast, both C_{TL} and C_{TR} increased substantially with temperature in the BSrf and ANrf soils. The large variation in soil C mineralization between parent materials again suggests a significant soil mineralogy control of soil C response to temperature.

Natural abundance $\delta^{13}C$ of mineralized CO₂

Rate model parameters suggest changes in the size of the labile and resistant pool with increasing temperature and possibly a shift in C source. A change in initial C source with increasing temperature is also suggested by a change in the $\delta^{13}CO_2$ signature of the respired CO₂ at the beginning of the incubation (Fig. 2). Figure 2 demonstrates the typical shift in $\delta^{13}CO_2$ with temperature observed among all biomes over time. Using the initial $\delta^{13}CO_2$ signature as a proxy for the $\delta^{13}C$ signature of the labile soil C pool, we can speculate as to the nature of the soil C components utilized for metabolism by the microbial biomass in the early stages of the incubation. At 5.0 °C, respired CO₂ is enriched in $\delta^{13}C$ (approximately -24‰ to -26‰), suggesting decomposition of ¹³C-enriched labile biomolecules, such as carbohydrates or polysaccharides (Benner *et al.*, 1987) or possible recycling of microbial biomass with minimal

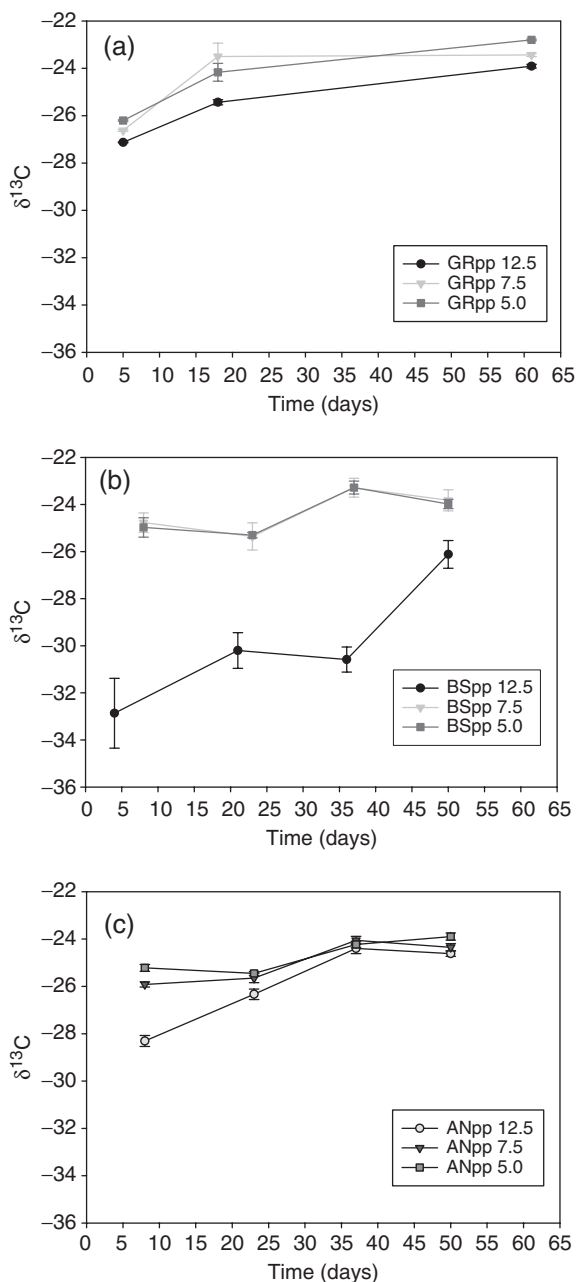


Fig. 2 Change in $\delta^{13}\text{C}$ of respired CO_2 over time for (a) GRpp (granite parent material, ponderosa pine biome), (b) BSpp (basalt parent material, ponderosa pine biome), and (c) ANpp (andesite parent material, ponderosa pine biome) temperature treatments. Closed circles, triangles, and squares represent the 12.5 °C, 7.5 °C, and 5.0 °C treatments, respectively. Error bars represent the standard error calculated for the mean $\delta^{13}\text{CO}_2$ value of four composite replicates.

soil C utilization. At 12.5 °C, $\delta^{13}\text{CO}_2$ is relatively depleted (approximately -33‰ to -28‰), suggesting greater utilization of more recalcitrant, phenolic or

lignin-like components (Benner *et al.*, 1987). Similarly, Andrews *et al.* (2000) observed that the $\delta^{13}\text{C}$ of respired soil CO_2 showed a 2.5–3.5 per mil enrichment at 4 °C relative to 22 °C and 40 °C, respectively, and suggested a change in primary C source utilization with temperature. The shift in $\delta^{13}\text{CO}_2$ corresponded with a shift in microbial community and species richness, suggesting temperature-controlled microbial community structure (Andrews *et al.* 2000). Microbial communities differ in their capacity to produce oxidative enzymes, such that a shift in microbial community with temperature may provide a mechanism for enhanced degradation of older, more recalcitrant, ^{13}C -depleted soil C at higher temperatures (Waldrop & Firestone, 2004).

Over time, the temperature treatments converge, and the final $\delta^{13}\text{CO}_2$ is similar between temperature treatments and parent materials (approximately -24‰) (Fig. 2). This change in $\delta^{13}\text{CO}_2$ over time is likely due to a shift in C source and greater recycling of microbial byproducts, rather than use of unaltered soil C components. This experiment did not include any litter addition (outside of any litter material that may have been included after sieving at 2 mm), such that any labile soil C components would have been decomposed or assimilated into the microbial biomass early in the incubation. Toward the end of the experiment, the microbial biomass may represent the most labile source of C.

Summary

Our results demonstrate that soil mineralogy moderates soil C mineralization within similar biomes, and soil C mineralization response to temperature. In particular, our data indicate significant differences in soil C mineralization between soils dominated by SRO minerals and those dominated by 1:1 and 2:1 phyllosilicates. Soils dominated by 2:1 and 1:1 minerals exhibited greater total soil C mineralization and a dominance of soil C dynamics by labile pools, suggesting possible significant loss of soil C or change in soil C dynamics in these soils under a climate warming scenario. The lack of protection in these soils may be a function of reduced surface area and aggregate formation potential that would physically protect soil C from decomposition. In contrast, soils dominated by SRO minerals mineralized very little C and were dominated by resistant soil C pools. The lack of C mineralization in these soils is most likely controlled by physical adsorption of soil C to mineral surfaces, rendering them unavailable for decomposition. In particular, AN soil C appears to be well buffered against changes in temperature, suggesting minimal loss of soil C under climate warming scenarios.

We also observed changes in pool size, initial decomposition rate, and CO₂ ¹³C signature with increasing temperature of incubation and by parent material, suggesting an interactive control of soil mineralogy and temperature on the ability of the microbial population to access soil C pools or substrates. Specifically, at cold temperatures, CO₂ was enriched in ¹³C, suggesting a preference for more labile carbohydrate/polysaccharide components, whereas more recalcitrant lignin like materials were increasingly utilized as a C source with increasing temperature. The shift to larger pools supports this shift in C source utilization and decomposition of more recalcitrant material at warmer temperatures. The changes in pool size and initial decomposition rate constants varied with soil mineral assemblage, further suggesting that biome soil C response to temperature change is not uniform within a biome, but is controlled in part by the soil mineral assemblage.

Our results suggest that regional models of soil C response to climate change cannot rely solely on clay content and vegetation type to estimate climate change effects on soil C stocks. The dramatic differences in soil C response to temperature by parent material suggest that soil mineralogy, specifically SRO Al- and Fe-oxyhydroxide and Al-humus complex content, should be integrated into current biogeochemical models in order to more accurately assess soil C response to temperature.

Acknowledgements

This work was funded through USDA Cooperative Agreement No 68-7482-7-240. Supplemental funding was provided through the U.C. Davis Jastro-Shields Fellowship program, with funds awarded to Craig Rasmussen. We thank David Harris and the U.C. Davis Stable Isotope Facility for processing samples for stable isotope analyses and assistance with analyzing stable isotope data. We also thank Tomer Shetrit for laboratory assistance, as well as Timothy Doane, and Thais Winsome for advice on incubation setup and laboratory procedures.

References

Anderson DW (1995) The role of nonliving organic matter in soils. In: *The Role of Nonliving Organic Matter in the Earth's Carbon Cycle* (eds Zepp RG, Sontag CH), pp. 81–92. John Wiley & Sons, New York.

Andrews JA, Matamala R, Westover KM *et al.* (2000) Temperature effects on the diversity of soil heterotrophs and the delta C-13 of soil-respired CO₂. *Soil Biology and Biochemistry*, **32**, 699–706.

Baldock JA, Skjemstad JO (2000) Role of the soil matrix and minerals in protecting natural organic materials against biological attack. *Organic Geochemistry*, **31**, 697–710.

Balesdent J, Mariotti A (1996) Measurement of soil organic matter turnover using ¹³C natural abundance. In: *Mass*

Spectrometry of Soils (eds Boutton T, Yamasaki S), pp. 83–112. Marcel Dekker, Inc., New York.

Benner R, Fogel ML, Sprague EK *et al.* (1987) Depletion of C-13 in lignin and its implications for stable carbon isotope studies. *Nature*, **329**, 708–710.

Boudot JP (1992) Relative efficiency of complexed aluminum, noncrystalline Al hydroxide, allophane and imogolite in retarding the biodegradation of citric-acid. *Geoderma*, **52**, 29–39.

Dahlgren RA (1994) Quantification of allophane and imogolite. In: *Quantitative Methods in Soil Mineralogy* (eds Amonette JE, Zelazny LW), pp. 430–451. Soil Science Society of America Inc., Madison, WI.

Dahlgren RA, Boettinger JL, Huntington GL *et al.* (1997) Soil development along an elevational transect in the western Sierra Nevada, California. *Geoderma*, **78**, 207–236.

Dalias P, Anderson JM, Bottner P *et al.* (2001) Long-term effects of temperature on carbon mineralisation processes. *Soil Biology and Biochemistry*, **33**, 1049–1057.

Dalias P, Kokkoris GD, Troumbis AY *et al.* (2003) Functional shift hypothesis and the relationship between temperature and soil carbon accumulation. *Biology and Fertility of Soils*, **37**, 90–95.

Devevre OC, Horwath WR (2000) Decomposition of rice straw and microbial carbon use efficiency under different soil temperatures and moistures. *Soil Biology and Biochemistry*, **32**, 1773–1785.

Ellert BH, Bettany JR (1988) Comparison of kinetic-models for describing net sulfur and nitrogen mineralization. *Soil Science Society of America Journal*, **52**, 1692–1702.

Guggenberger G, Haider KM (2002) Effect of mineral colloids on biogeochemical cycling of C, N, P and S in soil. In: *Interactions between Soil Particles and Microorganisms: Impact on the Terrestrial Ecosystem*, Vol. 8 (eds Huang PM, Bollag JM, Senesi N), pp. 267–322. John Wiley and Sons, Ltd., New York.

Harsh JB, Chorover J, Nizeyimana E (2002) Allophane and imogolite. In: *Soil Mineralogy with Environmental Applications* (eds Dixon JB, Schulze DG), pp. 291–321. Soil Science Society of America, Inc., Madison.

Hess TF, Schmidt SK (1995) Improved procedure for obtaining statistically valid parameter estimates from soil respiration data. *Soil Biology and Biochemistry*, **27**, 1–7.

Homann PS, Sollins P, Fiorella M *et al.* (1998) Regional soil organic carbon storage estimates for western Oregon by multiple approaches. *Soil Science Society of America Journal*, **62**, 789–796.

Illmer P, Obertegger U, Schinner F *et al.* (2003) Microbiological properties in acidic forest soils with special consideration of KCl extractable Al. *Water, Air and Soil Pollution*, **148**, 3–14.

Jackson ML (1975) *Soil Chemical Analysis Advanced Course*, 2nd edn. Jackson ML, Madison, WI.

Jardine PM, Weber NL, McCarthy JF *et al.* (1989) Mechanisms of dissolved organic-carbon adsorption on soil. *Soil Science Society of America Journal*, **53**, 1378–1385.

Jones DL, Edwards AC (1998) Influence of sorption on the biological utilization of two simple carbon substrates. *Soil Biology and Biochemistry*, **30**, 1895–1902.

Lenihan JM, Drapek R, Bachelet D *et al.* (2003) Climate change effects on vegetation distribution, carbon, and fire in California. *Ecological Applications*, **13**, 1667–1681.

MacDonald NW, Zak DR, Pregitzer KS *et al.* (1995) Temperature effects on kinetics of microbial respiration and net nitrogen

- and sulfur mineralization. *Soil Science Society of America Journal*, **59**, 233–240.
- Martin JP, Haider K (1986) Influence of mineral colloids on turnover rates of soil organic carbon. In: *Interactions of Soil Minerals with Natural Organics and Microbes* (eds Huang PM, Schnitzer M), pp. 283–304. Soil Science Society of America, Inc., Madison.
- Miltner A, Zech W (1998) Carbohydrate decomposition in beech litter as influenced by aluminium, iron and manganese oxides. *Soil Biology and Biochemistry*, **30**, 1–7.
- [NAST] National Assessment Synthesis Team (2000) *Climate Change Impact on the United States: The Potential Consequences of Climate Variability and Change*. Cambridge University Press, New York.
- National Soil Survey Laboratory (1996) *Soil survey laboratory methods manual*. Soil Survey Investigations Report No. 42, Version 3.0. United States Department of Agriculture, Natural Resources Conservation Service, National Soil Survey Center, Lincoln, NE.
- Oades JM (1988) The retention of organic-matter in soils. *Biogeochemistry*, **5**, 35–70.
- Parfitt RL (1980) Chemical properties of variable charge soils. In: *Soils with Variable Charge* (ed Theng BKG), pp. 167–194. Soil Bureau, Lower Hutt, New Zealand.
- Parfitt RL, Childs CW (1988) Estimation of forms of Fe and Al – a review, and analysis of contrasting soils by dissolution and Mossbauer methods. *Australian Journal of Soil Research*, **26**, 121–144.
- Parfitt RL, Parshotam A, Salt GJ *et al.* (2002) Carbon turnover in two soils with contrasting mineralogy under long-term maize and pasture. *Australian Journal of Soil Research*, **40**, 127–136.
- Parton WJ, Schimel DS, Cole CV *et al.* (1987) Analysis of factors controlling soil organic-matter levels in Great-Plains grasslands. *Soil Science Society of America Journal*, **51**, 1173–1179.
- Paul EA, Clark FE (1996) *Soil Microbiology and Biochemistry*, 2nd edn. Academic Press, San Diego.
- Percival HJ, Parfitt RL, Scott NA *et al.* (2000) Factors controlling soil carbon levels in New Zealand grasslands: Is clay content important? *Soil Science Society of America Journal*, **64**, 1623–1630.
- Rasmussen C, Torn MS, Southard RJ *et al.* (2005) Mineral assemblage and aggregates control carbon dynamics in a California conifer forest. *Soil Science Society of America Journal*, **69**, 1711–1721.
- Saggar S, Tate KR, Feltham CW *et al.* (1994) Carbon turnover in a range of allophanic soils amended with C-14-labeled glucose. *Soil Biology and Biochemistry*, **26**, 1263–1271.
- Saggar S, Parshotam A, Sparling GP *et al.* (1996) C-14-labelled ryegrass turnover and residence times in soils varying in clay content and mineralogy. *Soil Biology and Biochemistry*, **28**, 1677–1686.
- Schlesinger W (1997) *Biogeochemistry*. Academic Press, San Diego, CA.
- Schwesig D, Kalbitz K, Matzner E *et al.* (2003) Effects of aluminium on the mineralization of dissolved organic carbon derived from forest floors. *European Journal of Soil Science*, **54**, 311–322.
- Shafer SL, Bartlein PJ, Thompson RS *et al.* (2001) Potential changes in the distributions of western North America tree and shrub taxa under future climate scenarios. *Ecosystems*, **4**, 200–215.
- Shang C, Tiessen H (1998) Organic matter stabilization in two semiarid tropical soils: size, density, and magnetic separations. *Soil Science Society of America Journal*, **62**, 1247–1257.
- Shoji S, Nanzyo M, Dahlgren RA (1993) *Volcanic Ash Soils: Genesis, Properties and Utilization*. Developments in Soil Science. No. 21. Elsevier, Amsterdam.
- Six J, Elliott ET, Paustian K *et al.* (2000) Soil structure and soil organic matter: II. A normalized stability index and the effect of mineralogy. *Soil Science Society of America Journal*, **64**, 1042–1049.
- Soil Survey Staff (2003) *Keys to Soil Taxonomy*, 9th edn. USDA Natural Resources Conservation Service, Washington, DC.
- Stevenson FJ (1994) *Humus Chemistry: Genesis, Composition, Reactions*. John Wiley & Sons, Inc., New York, NY.
- Tate KR, Theng BKG (1980) Organic matter and its interactions with inorganic soil constituents. In: *Soils with Variable Charge* (ed Theng BKG), pp. 225–252. Soil Bureau, Lower Hutt, New Zealand.
- Taylor BR, Parkinson D (1988) Respiration and mass-loss rates of aspen and pine leaf litter decomposing in laboratory microcosms. *Canadian Journal of Botany-Revue Canadienne De Botanique*, **66**, 1948–1959.
- Torn MS, Trumbore SE, Chadwick OA *et al.* (1997) Mineral control of soil organic carbon storage and turnover. *Nature*, **389**, 170–173.
- Trumbore SE, Chadwick OA, Amundson RA *et al.* (1996) Rapid exchange between soil carbon and atmospheric carbon dioxide driven by temperature change. *Science*, **272**, 393–396.
- Veldkamp E (1994) Organic-carbon turnover in three tropical soils under pasture after deforestation. *Soil Science Society of America Journal*, **58**, 175–180.
- Waldrop MP, Firestone MK (2004) Altered utilization patterns of young and old soil C by microorganisms caused by temperature shifts and N additions. *Biogeochemistry*, **67**, 235–248.
- Whittig LD, Allardice WR (1986) X-ray diffraction techniques. In: *Methods of Soil Analysis – Part I. Physical and Mineralogical Methods* (ed Klute A), pp. 331–362. Soil Science Society of America Inc., Madison, WI.
- Yuan G, Theng BKG, Parfitt RL *et al.* (2000) Interactions of allophane with humic acid and cations. *European Journal of Soil Science*, **51**, 35–41.
- Zak DR, Holmes WE, MacDonald NW *et al.* (1999) Soil temperature matric potential and the kinetics of microbial respiration and nitrogen mineralization. *Soil Science Society of America Journal*, **63**, 475–481.
- Zibilske LM (1994) Carbon Mineralization. In: *Methods of Soil Analysis Part 2 Microbiological and Biochemical Properties* (eds Weaver RW, Angle S, Bottomley P), pp. 835–864. Soil Science Society of America, Inc., Madison, WI.
- Zogg GP, Zak DR, Ringelberg DB *et al.* (1997) Compositional and functional shifts in microbial communities due to soil warming. *Soil Science Society of America Journal*, **61**, 475–481.
- Zunino H, Borie F, Aguilera S *et al.* (1982) Decomposition of C-14-labeled glucose, plant and microbial products and phenols in volcanic ash-derived soils of Chile. *Soil Biology and Biochemistry*, **14**, 37–43.